The 5th Joint International Conference on Multibody System Dynamics
June 24 – 28, 2018, Lisboa, Portugal

# Set-Based Design of Automobile Independent Suspension Linkages

David Kline[1] and Gregory Hulbert[1]

[1]*Mechanical Engineering, University of Michigan, {delkline,hulbert}@umich.edu*

ABSTRACT — *The independent suspension linkage allows each wheel of an automobile to move approximately vertically relative to the vehicle body without affecting the motion of the other wheels. The wheel trajectory itself, which is established by the linkage type/geometry, has implications on the performance, comfort, and safety of the automobile. For any given linkage type, geometric design relies on iterating a draft geometry until the suspension performs acceptably. This process makes evaluating one linkage type, let alone many, tedious and expensive. Additionally, the iterative design process does not make clear potential conceptual issues with the design problem as it is posed. Is the desired wheel trajectory even mathematically possible? How much of the desired trajectory, if any, is the selected linkage type capable of achieving? To address these questions, we propose a set-based design approach for independent suspension linkages. After specifying a mathematically-complete wheel trajectory, all possible linkage types are evaluated conceptually. Types never capable of achieving satisfactory performance are pruned. Next, the geometries of the remaining types are directly synthesized, producing families of geometries which produce the desired motion. Requirements other than wheel trajectory (e.g., allotted space, provisions for a steering axis, minimization of link reaction loads) are then used to further cut down the solution space. Examples are provided which demonstrate the efficacy of the methods, including the complete synthesis of a linkage consisting of five spherical-spherical links. Key to the success of these methods is the wheel motion formalism developed herein, allowing curves in $SE(3)$, the group of spatial rigid body motions, to be defined in terms of kinematic suspension characteristics, e.g., camber angle, toe angle, and roll center height.*

## 1 Introduction

The independent suspension allows each wheel of an automobile to move approximately vertically relative to the vehicle body without affecting the motion of the other wheels. It consists primarily of a linkage connecting the wheel carrier to the vehicle body, a spring, and a damper (or shock). The linkage is responsible for guiding the wheel along the desired trajectory, providing the vertical degree-of-freedom upon which the spring and damper act to support the vehicle body and isolate it from road irregularities [1, Ch. 4]. Nowadays, independent suspensions are designed when an existing vehicle is in need of improved performance, or when a new vehicle is developed. From vehicle-level ride-and-handling requirements, experienced designers select a suspension architecture (linkage type) which is potentially suitable. Next, designers create a draft linkage geometry which fits inside the allotted space for the linkage, and iterate its dimensions until it guides the wheel satisfactorily. The spring and damper themselves are then located and their properties selected. Vehicle-level testing and tuning completes the suspension's development, including the addition of mounts and bushings to improve suspension performance. This approach to suspension design is classified as point-based design, in that it is characterized by choosing a solution and then iterating until a better solution is found. Architecture selection and geometry selection are portions of suspension design particularly suited to a different approach, namely set-based design. There exists the obvious possibility of a designer selecting an architecture which will never meet the desired wheel trajectory. Moreover, the geometric design process is tedious, requiring even an experienced designer to run simulations dozens of times [2]. Fortunately, kinematicians have long worked on methods to systematically enumerate linkage types and solve directly for link dimensions based on the kinematic requirements [3, 4]. Rather than choosing one suspension

architecture based on experience, a set of candidate architectures can be enumerated [5]. Rather than choosing one geometry and iterating it, a family of geometries that achieve the desired motion can be found [6, 7, 8]. In this way, a large number of possible suspension linkages can be produced, some of which can then be eliminated by subsequent concerns, leaving only the viable design solutions, thus following a set-based design process.

In pursuing a set-based design approach for independent suspension linkages, we identified four areas in need of attention: (1) wheel motion specification, (2) catalog of linkage types, (3) dimensional synthesis methods, and (4) methods used for pruning solutions according to non-kinematic requirements. As an example of the need for work on the wheel motion specification, *roll center height* is a characteristic associated with body roll during cornering; its definition includes the velocity vector of the tire contact point. It should be possible to define a curve in $SE(3)$, the group of spatial rigid body motions, in terms of application-specific characteristics like roll center height. Previous attempts at achieving desired roll center height behavior relied on architecture-specific rules [9], which are unsuitable for set-based design, since we do not wish to assume a particular architecture *a-priori*. While there exists an exhaustive catalog of possible suspension linkage types [5], this number synthesis includes some impractical joints and links. A much smaller, yet highly useful, enumeration is possible by merely considering the joints and links used in practice. In the auto industry, dimensional synthesis, where various point and line coordinates are computed based on the motion specification, still is reliant on graphical methods for the draft geometry and iteration thereafter [10, 11, 6]. On the other hand, algebraic methods, better suited to automated computation, are commonplace in the general kinematics literature [3, 4]. The most complete treatment of these methods for suspension linkages is limited to those in the plane [8]. An area of geometric design unique to the suspension linkage is the need to trade-off wheel kinematics for other considerations such as allotted space and provisions for a steering axis. In the general geometric design literature mentioned previously, the focus is on solving linkage design equations for the maximum number of specifiable body positions. The desire to reduce the number of specified positions to enable other aspects of the design is overwhelming for suspension designers, hence a clear need for work on systematic ways to handle these under-specified problems.

The body of this paper is organized into four main sections, each corresponding to an area in need of attention: wheel kinematics, linkage types, dimensional synthesis, and non-kinematic design considerations. Examples will be introduced in each section that demonstrate the methods and efficacy of the set-based approach.

# 2 Wheel Kinematics

## 2.1 Preliminaries

We identify vectors in Euclidean space with $\mathbb{R}^3$ in the usual way, writing their components with respect to a right-handed, orthonormal basis. We write these down as *column vectors* ($3 \times 1$ matrices). We also fix an origin of Euclidean space, so we can identify points with their position vectors, and, ultimately, their column vectors, which we call *coordinate vectors* in this context. In terms of coordinate vectors, an isometry is a function $\mathbb{R}^3 \to \mathbb{R}^3$ given by

$$\mathbf{x} \mapsto \mathbf{A}\mathbf{x} + \mathbf{b},$$

where $\mathbf{A}$ is an orthogonal matrix — that is, $\mathbf{A}^T\mathbf{A} = \mathbf{A}\mathbf{A}^T = \mathbf{I}$, where $\mathbf{I}$ is the $3 \times 3$ identity matrix — and $\mathbf{b}$ is a column vector. A direct isometry has $\det \mathbf{A} = +1$, while an indirect isometry has $\det \mathbf{A} = -1$. Orthogonal matrices with determinant $+1$ are called *special orthogonal* matrices.

Examples of direct isometries include rotations and translations. Translations are straightforward: we move points the direction and distance given by a vector. In terms of coordinate vectors, the *translation by a (column) vector* $\mathbf{v}$ is the function $\mathbb{R}^3 \to \mathbb{R}^3$ given by $\mathbf{x} \mapsto \mathbf{x} + \mathbf{v}$. In this context, a *rotation* is one about an axis through the origin. In particular, let $\theta$ be an angle and $\mathbf{u} = (u_1, u_2, u_3)^T$ a column vector of unit length giving the direction of the axis, which gives the direction of the rotation by the right-hand rule. In terms of coordinate vectors, the *rotation through angle $\theta$ with axis through the origin in direction* $\mathbf{u}$ is the function $\mathbb{R}^3 \to \mathbb{R}^3$ defined by $\mathbf{x} \mapsto \mathbf{R}_{\mathbf{u},\theta}\mathbf{x}$, where

$$\mathbf{R}_{\mathbf{u},\theta} = \mathbf{I} + \sin\theta\tilde{\mathbf{u}} + (1 - \cos\theta)\tilde{\mathbf{u}}^2, \tag{1}$$

where $\tilde{\mathbf{u}}$ is the skew-symmetric matrix

$$\tilde{\mathbf{u}} = \begin{pmatrix} 0 & -u_3 & u_2 \\ u_3 & 0 & -u_1 \\ -u_2 & u_1 & 0 \end{pmatrix}.$$

These matrices arise from writing the cross product of two vectors as a matrix-vector product; in particular, given $\mathbf{u} \in \mathbb{R}^3$, for all $\mathbf{v} \in \mathbb{R}^3$ we have

$$\mathbf{u} \times \mathbf{v} = \tilde{\mathbf{u}}\mathbf{v}.$$

The *trajectory*, or *continuous motion* of a rigid body can be modeled with a time-varying family of direct isometries, with the isometry at a particular instant being the one that takes the body from the original position to the current position. (As such, the identity isometry given by orthogonal matrix $\mathbf{I}$ and column vector $\mathbf{0}$ must be included.) Suppose we have such a family of direct isometries, where $\mathbf{A}(t)$ and $\mathbf{b}(t)$ are the orthogonal matrix and the column vector, respectively, of the direct isometry at time $t$. A point on the body with coordinate vector $\mathbf{x}_0$ in the body's original position has coordinate vector

$$\mathbf{x}(t) = \mathbf{A}(t)\mathbf{x}_0 + \mathbf{b}(t)$$

at time $t$. The velocity of the point on the body with coordinate vector $\mathbf{x}(t)$ is

$$\mathbf{v}_{\mathbf{x}}(t) = \boldsymbol{\omega}(t) \times \mathbf{x}(t) + \mathbf{v}(t),$$

where $\boldsymbol{\omega}(t)$ is the angular velocity of the body, arising from

$$\tilde{\boldsymbol{\omega}}(t) = \dot{\mathbf{A}}(t)(\mathbf{A}(t))^T,$$

and $\mathbf{v}(t)$ is the velocity of the point on the body which is currently passing through the origin, given by

$$\mathbf{v}(t) = \dot{\mathbf{b}}(t) - \boldsymbol{\omega}(t) \times \mathbf{b}(t).$$

## 2.2 Wheel Position

We wish to model the wheel of a passenger car as a body which moves with respect to a fixed vehicle body. Both of these bodies are assumed to be rigid. By *wheel*, we mean the combined wheel and wheel carrier assembly, ignoring the possibility of relative rotation between these two (this is the typical assumption employed in the early design stage). To this end, we identify the vehicle body in Euclidean space. The origin is defined as the intended location of the center of a right-hand side wheel when the vehicle is at its design load, and the standard basis vectors $\mathbf{i} = (1,0,0)^T$, $\mathbf{j} = (0,1,0)^T$, and $\mathbf{k} = (0,0,1)^T$ have the following meaning: $\mathbf{i}$ aims in the forward driving direction, $\mathbf{j}$ aims to the driver's left-hand side, and $\mathbf{k}$ aims upward. The wheel is modeled as a disk with radius $r$, and it is in the *design position* when its center is at the origin and it is normal to the vector $\mathbf{j}$. The ground is modeled as a $\mathbf{k}$-normal plane which translates vertically so that it always contains the lowest-hanging point of the wheel. In the design position, the circumference of the wheel can be given by

$$\{(r\sin\psi, 0, -r\cos\psi)^T : -\pi < \psi \leq \pi\}. \tag{2}$$

The lowest-hanging point is given by $\psi = 0$, corresponding to coordinate vector $(0,0,-r)^T$.

We wish to give a convenient form of general wheel motion from the design position. Since the wheel is assumed to be rigid, in general its motion is described by direct isometries. It is well known that any orientation of a (rigid) body about the origin can be achieved by composing three rotations about three mutually perpendicular axes through the origin. In particular, the wheel can first be rotated by angle $\phi$ about the $y$-axis, which has direction $\mathbf{j}$, then by angle $\gamma$ about the $x$-axis, which has direction $\mathbf{i}$, and finally rotated by angle $\delta$ about the $z$-axis, which has direction $\mathbf{k}$. These rotations are visualized in Figure 1. Valid intervals for angles $\phi$, $\gamma$, and $\delta$ are considered to be

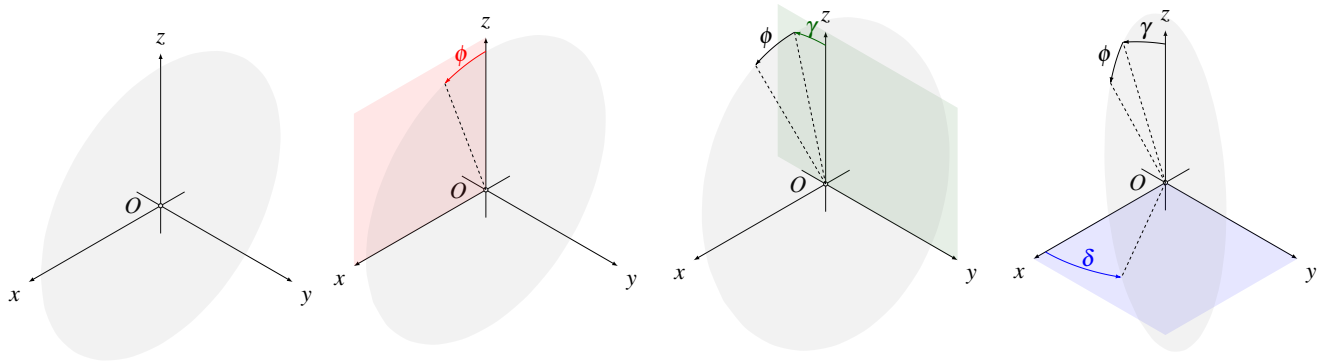


(a) Design position.

(b) Rotate by $\phi$ about the $y$-axis.

(c) Rotate by $\gamma$ about the $x$-axis.

(d) Rotate by $\delta$ about the $z$-axis.

Fig. 1: Orienting the wheel with three rotations.

$$I_\phi = \{\phi \in \mathbb{R} : -\pi < \phi \leq \pi\},$$
$$I_\gamma = \{\gamma \in \mathbb{R} : -\pi/2 \leq \gamma \leq \pi/2\},$$
$$I_\delta = \{\delta \in \mathbb{R} : -\pi < \delta \leq \pi\}.$$

These intervals are sufficient for the wheel to reach any orientation. This representation of orientation is unique except when $\gamma = \pm\pi/2$. In this case, we cannot tell the difference between $\delta$ and $\phi$. Finally, any spatial position of the wheel can be reached by translating the oriented wheel by some vector $(x,y,z)^T$. Altogether a *wheel motion* acts on coordinate vectors as

$$\mathbf{x} \mapsto \mathbf{R}_{\mathbf{k},\delta}\mathbf{R}_{\mathbf{i},\gamma}\mathbf{R}_{\mathbf{j},\phi}\mathbf{x} + (x,y,z)^T.$$

This parameterization of direct isometries is convenient because the parameters $\phi$, $\gamma$, $\delta$, $x$, $y$, and $z$ have meaning in an automotive context:

- The angle $\phi$ is the *spin angle* of the wheel. It is is positive when the wheel (and carrier fixed to it!) rotates as if it rolled forward.
- The angle $\gamma$ is the *camber angle* of the wheel. It is positive when the top of the wheel rotates away from the vehicle body and negative when the top of the wheel rotates toward the vehicle body. As stated before, the parameterization is not unique when the camber angle is $\pm\pi/2$, because it cannot distinguish between $\delta$ and $\phi$. (We would never expect a wheel to get anywhere near a camber angle of $\pm\pi/2$.)
- The angle $\delta$ is the *toe angle* of the wheel. It is positive when the front of the wheel rotates toward the vehicle body (*toe-in*) and negative when the front of the wheel rotates away from the vehicle body (*toe-out*).

For the other parameters, recall that in the design position, the wheel center coincides with the origin. The parametrized isometry maps this to the point with coordinate vector $(x,y,z)^T$. We see the following:

- The coordinate $x$ is the *longitudinal displacement* of the wheel center. It is positive when the wheel moves toward the front of the vehicle.
- The component $y$ is the *lateral displacement* of the wheel center. It is positive when the wheel moves to the left side of the vehicle.
- The component $z$ is the *vertical displacement* of the wheel center. It is positive when the wheel moves up. When $z > 0$ the wheel is said to be in *jounce* and when $z < 0$ the wheel is said to be in *rebound*.

Of interest is the location of the ground plane after the wheel moves. Recall the parametric form of a point on the circumference of the wheel in the design position, (2). The wheel isometry maps this to

$$\begin{pmatrix} x - r\sin(\phi-\psi)\cos\delta - r\cos(\phi-\psi)\sin\delta\sin\gamma \\ y - r\sin(\phi-\psi)\sin\delta + r\cos(\phi-\psi)\cos\delta\sin\gamma \\ z - r\cos(\phi-\psi)\cos\gamma \end{pmatrix},$$

where some trigonometric identities have been used. In order to have a unique lowest-hanging point, we assume that $-\pi/2 < \gamma < \pi/2$. We then focus on finding $\psi$ such that $\cos(\phi-\psi) = 1$. The obvious solution here is just $\psi = \phi$. Thus, the lowest-hanging point on the wheel (the *tire contact point*) after a wheel motion is

$$\begin{pmatrix} x - r\sin\delta\sin\gamma \\ y + r\cos\delta\sin\gamma \\ z - r\cos\gamma \end{pmatrix}. \tag{3}$$

### 2.3 Wheel Velocity

An independent suspension linkage is designed to constrain the wheel so that there is only one degree of freedom (DOF). We assume that wheel center vertical displacement $z$ drives the other five DOFs of the rigid wheel. In particular, let $z$ take values in the interval $I_z$, which is assumed to contain zero. Then, we assume that $\phi : I_z \to (-\pi, \pi]$, $\gamma : I_z \to [-\pi/2, \pi/2]$, $\delta : I_z \to (-\pi, \pi]$, $x : I_z \to \mathbb{R}$, $y : I_z \to \mathbb{R}$ are differentiable functions which satisfy

$$\phi(0) = \gamma(0) = \delta(0) = x(0) = y(0) = 0.$$

The trajectory of the wheel is thus described by the $z$-varying family of direct isometries with special orthogonal matrix

$$\mathbf{A}(z) = \mathbf{R}_{\mathbf{k},\delta(z)}\mathbf{R}_{\mathbf{i},\gamma(z)}\mathbf{R}_{\mathbf{j},\phi(z)}$$

and column vector

$$\mathbf{b}(z) = (x(z), y(z), z)^T.$$

Notice that the original, design position of the wheel corresponds to $z = 0$.

The angular velocity of the wheel at vertical displacement $z$ arises from

$$\tilde{\boldsymbol{\omega}}(z) = \mathbf{A}'(z)(\mathbf{A}(z))^T;$$

where the prime mark denotes the derivative with respect to $z$, and, in particular, omitting dependencies on $z$ for brevity,

$$\boldsymbol{\omega} = \begin{pmatrix} \gamma'\cos\delta - \phi'\cos\gamma\sin\delta \\ \gamma'\sin\delta + \phi'\cos\delta\cos\gamma \\ \delta' + \phi'\sin\gamma \end{pmatrix}.$$

The velocity of the point on the wheel which is passing through the origin at vertical displacement $z$ is given by

$$\mathbf{v}(z) = \mathbf{b}'(z) - \boldsymbol{\omega}(z) \times \mathbf{b}(z).$$

Again omitting dependencies on $z$,

$$\mathbf{v} = \begin{pmatrix} x' + \delta' y - \gamma' z\sin\delta + \phi'(y\sin\gamma - z\cos\delta\cos\gamma) \\ y' - \delta' x + \gamma' z\cos\delta - \phi'(x\sin\gamma + z\sin\delta\cos\gamma) \\ \gamma'(x\sin\delta - y\cos\delta) + \phi'\cos\gamma(x\cos\delta + y\sin\delta) + 1 \end{pmatrix}.$$

Several suspension characteristics are defined from the wheel's velocity. In particular, we are interested in the wheel center velocity and the contact point velocity. We continue to not write dependencies on $z$. At vertical displacement $z$, the wheel center has coordinate vector

$$\mathbf{b} = (x, y, z)^T.$$

The velocity of the point on the wheel with that coordinate vector is

$$\begin{aligned}\mathbf{v_b} &= \boldsymbol{\omega} \times \mathbf{b} + \mathbf{v} \\ &= \boldsymbol{\omega} \times \mathbf{b} + \mathbf{b}' - \boldsymbol{\omega} \times \mathbf{b} \\ &= \mathbf{b}' \\ &= (x', y', 1)^T.\end{aligned}$$

Referring to (3), at vertical displacement $z$, the contact point, or lowest-hanging point of the wheel, has coordinate vector

$$\mathbf{c} := \begin{pmatrix} x - r\sin\delta\sin\gamma \\ y + r\cos\delta\sin\gamma \\ z - r\cos\gamma \end{pmatrix}.$$

The velocity of the point on the wheel with coordinate vector $\mathbf{c}$ is

$$\begin{aligned}\mathbf{v_c} &= \boldsymbol{\omega} \times \mathbf{c} + \mathbf{v} \\ &= \begin{pmatrix} x' - \phi' r\cos\delta - \delta' r\cos\delta\sin\gamma - \gamma' r\cos\gamma\sin\delta \\ y' - \phi' r\sin\delta + \gamma' r\cos\delta\cos\gamma - \delta' r\sin\delta\sin\gamma \\ \gamma' r\sin\gamma + 1 \end{pmatrix}.\end{aligned}$$

The vector $\mathbf{v}_c$ is the velocity of the particular point on the wheel which happens to be the contact point for that value of $z$, not the tangent vector of $\mathbf{c}$ at $z$; that is, $\mathbf{v}_c \neq \mathbf{c}'$. This is because the contact point is not a unique point of the wheel; it instead moves around the circumference in order to hang the lowest.

Two suspension characteristics are defined from the velocities $\mathbf{v_b}$ and $\mathbf{v_c}$ when considering a side ($\mathbf{j}$-normal) view of the wheel; see Figure 2a. The first is *wheel-travel angle* $\varepsilon$, which is the inclination of $\mathbf{v_b}$ to the vertical in this side view. In particular,

$$\tan\varepsilon = \frac{v_{b_1}}{v_{b_3}} = x'. \tag{4}$$

For a driven front wheel, positive values of $\varepsilon$ give an anti-lift effect; for a driven rear wheel, negative values of $\varepsilon$ give an anti-squat effect. The second characteristic here is *support angle* $\varepsilon^*$, which is the inclination of $\mathbf{v_c}$ to the vertical in this side view; in particular,

$$\tan\varepsilon^* = \frac{v_{c_1}}{v_{c_3}} = \frac{x' - \phi' r\cos\delta - \delta' r\cos\delta\sin\gamma - \gamma' r\cos\gamma\sin\delta}{\gamma' r\sin\gamma + 1}. \tag{5}$$

For an outboard-braked front wheel, positive values of $\varepsilon^*$ give an anti-dive effect. For an outboard-braked rear wheel, negative values of $\varepsilon^*$ give an anti-rise effect.

One suspension characteristic, *roll center height*, denoted by $h$, is defined from the velocity $\mathbf{v_c}$ when considering a front ($\mathbf{i}$-normal) view of the wheel; see Figure 2b. The roll center height is the signed distance from the ground plane to the point where the perpendicular of the front view projection of $\mathbf{v_c}$ intersects the centerline of the vehicle body. Letting $s$ denote the design position track width of the axle, we have that

$$\frac{h}{s/2 - c_2} = \frac{-v_{c_2}}{v_{c_3}}.$$

In particular,

$$h = \frac{-(y' - \phi' r\sin\delta + \gamma' r\cos\delta\cos\gamma - \delta' r\sin\delta\sin\gamma)}{\gamma' r\sin\gamma + 1} \times (s/2 - (y + r\cos\delta\sin\gamma)) \tag{6}$$

For background on wheel-travel angle, support angle, and roll center height, see [11].

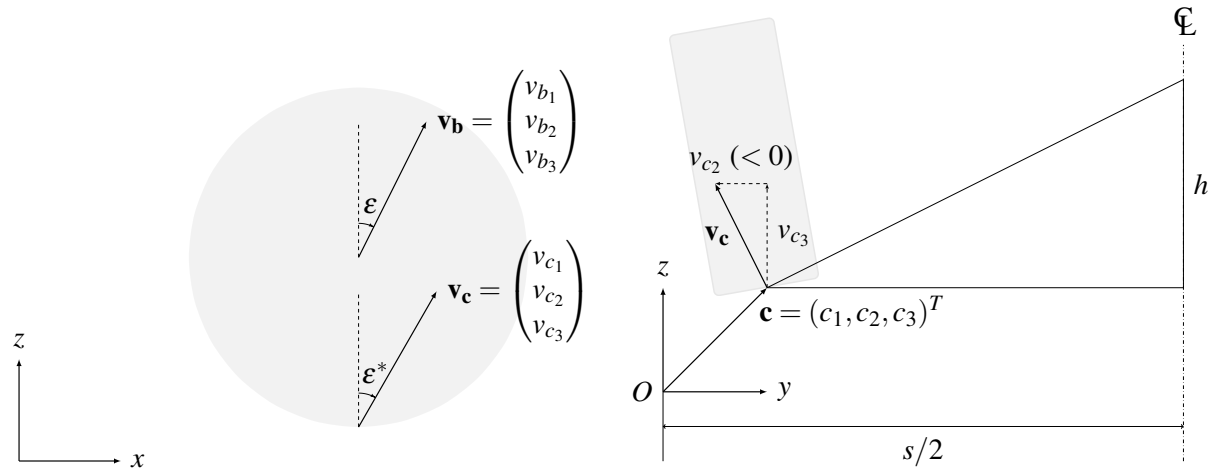


(a) Suspension characteristic definitions in the side view.

(b) Roll center height definition in the front view, with velocity component $v_{c_2}$ drawn negative to result in a positive roll center height $h$.

Fig. 2: Geometric definitions of velocity characteristics for suspensions.

## 2.4 Example Motion Specification

Let's consider a driven, outboard-braked rear wheel. We choose to define the $\gamma$, $\delta$, $\varepsilon$, $\varepsilon^*$, and $h$ curves, and deduce the remaining curves $x$, $y$ and $\phi$ from there. Throughout, length units are millimeters and angle units are radians. First, let

$$I_z = \{z \in \mathbb{R} : -99 \leq z \leq 99\},$$

wheel radius $r = 300$, and design position track width $s = 1400$. The camber function is defined by

$$\gamma(z) = (-1.5 \times 10^{-6})z^2 + \left(\frac{-0.5}{25.4}\frac{\pi}{180}\right)z,$$

giving progressively-negative camber in jounce. The toe function is defined by

$$\delta(z) = \left(0.005 \times \frac{\pi}{180}\right)z,$$

which gives a very slight roll understeer effect. Since we are working with a driven rear wheel, we want anti-squat behavior; consequently, we need negative values for the wheel-travel angle $\varepsilon$. Let

$$\varepsilon(z) = -6 \times \frac{\pi}{180}.$$

Similarly, since we have an outboard-braked rear wheel, we want anti-rise behavior, and thus negative values for support angle $\varepsilon^*$. Let

$$\varepsilon^*(z) = -15 \times \frac{\pi}{180}.$$

The roll center height is defined by

$$h(z) = 100 - (1)(z - r\cos\gamma(z) - (-r)),$$

which gives an initial roll center height of 100 mm, which decreases/increases by one times the amount the ground plane moves up/down. Determining the remaining $x$, $y$, and $\phi$ curves amounts to solving a few first order differential equations. In this way, a complete wheel trajectory can be specified from both position and velocity characteristics.

# 3 Linkage Types

A practical set of body-wheel connections is given by Matschinsky [11]. There are two categories: joints, which directly connect the wheel carrier to the vehicle body, and links, which have a joint on each end, producing an indirect connection. For independent suspensions, Matschinsky identifies three practical joints — revolute (R), cylindrical (C), and spherical (S) — and four practical links: S-S, R-S, R-R, and S-C. The R-R link is assumed to be spatial, having skew axes. The S-C link is such that the S joint lies on the C joint axis, implemented as the familiar damper strut. There is no systematic enumeration of connections which result in the wheel having one DOF; rather, example linkage types are presented. To perform a true number synthesis we consider combinations, repetition allowed, of connections which sum to remove five DOFs from the wheel. (Each connection is assumed to provide an independent set of constraints.) For this synthesis the number of DOFs removed from the wheel by each connection is needed; see Table 1.

| R | C | S | S-S | R-S | R-R | S-C |
|---|---|---|---|---|---|---|
| 5 | 4 | 3 | 1 | 2 | 4 | 2 |

Tab. 1: Number of DOFs removed by the practical body-wheel connections.

The seven integer partitions of five ($5$, $4+1$, $3+2$, $3+1+1$, $2+2+1$, $2+1+1+1$, $1+1+1+1+1$) suggest possible linkage types:

- 5. Only the R joint removes five DOFs directly.
- $4+1$. C and R-R remove four each. Only S-S removes one. Resulting linkages: C(S-S) and (R-R)(S-S). A linkage type is written as the "product" of its connections.
- $3+2$. Only S removes three. The R-S and S-C links remove two each. These links are reversible, so there are four possible linkage types here: S(R-S), S(S-R), S(S-C), S(C-S). We now consider the order of the joints in a link X-Y to be important; namely, X is on the body-side and Y is on the wheel-side.
- $3+1+1$ gives S(S-S)$^2$.
- $2+2+1$. Four connections remove two DOFs: R-S, S-R, S-C, and C-S. There are ten ways to choose two of these if repetition is allowed. These choices, together with an S-S link, form the following architectures: (R-S)$^2$(S-S), (R-S)(S-R)(S-S), (R-S)(S-C)(S-S), (R-S)(C-S)(S-S), (S-R)$^2$(S-S), (S-R)(S-C)(S-S), (S-R)(C-S)(S-S), (S-C)$^2$(S-S), (S-C)(C-S)(S-S), and (C-S)$^2$(S-S).
- $2+1+1+1$ implies four linkage types having three S-S links: (R-S)(S-S)$^3$, (S-R)(S-S)$^3$, (S-C)(S-S)$^3$, and (C-S)(S-S)$^3$.
- $1+1+1+1+1$ gives (S-S)$^5$.

In total there are 23 possible linkage types, some more practical than others. For instance, if the intent is to implement S-C and C-S links as damper struts, it is unlikely to have two such struts in one suspension. As such the (S-C)$^2$(S-S), (S-C)(C-S)(S-S), and (C-S)$^2$(S-S) architectures may be pruned. Even kinematic considerations can be used to prune architectures in this stage. Notice that any which use the R or S joint require a wheel motion from one pose to another to have a fixed point. If the desired wheel motion is a general rigid body motion, having no fixed points, the architectures R, S(R-S), S(S-R), S(S-C), S(C-S), and S(S-S)$^2$ may be pruned. No portion of the example motion specification of the previous section could be attainable with these architectures, but such a specification could be constructed if desired.

# 4 Dimensional Synthesis

In *dimensional synthesis*, the geometries of individual connections are synthesized according to the desired wheel trajectory. These geometric solutions can later be pruned if necessary and assembled into complete suspension linkages. The approach here is to formulate and solve so-called design equations.

## 4.1 Design Equations

The algebraic approach to dimensional synthesis relies on the implicit kinematic constraints that can be written for each of the joints and links in the catalog. For example, the S-S link constraint amounts to a constant distance between the body-side S joint and the wheel-side S joint. If $\mathbf{x}_0 \in \mathbb{R}^3$ is the wheel-side joint coordinate and $\mathbf{x}_1 \in \mathbb{R}^3$ is the body-side joint coordinate, then a wheel motion given by $\mathbf{A} \in SO(3)$ and $\mathbf{b} \in \mathbb{R}^3$ must satisfy

$$(\mathbf{A}\mathbf{x}_1 + \mathbf{b} - \mathbf{x}_0) \cdot (\mathbf{A}\mathbf{x}_1 + \mathbf{b} - \mathbf{x}_0) = (\mathbf{x}_1 - \mathbf{x}_0) \cdot (\mathbf{x}_1 - \mathbf{x}_0). \tag{7}$$

To construct *design equations*, we treat the joint coordinates as *design variables* for known wheel motion(s). For example, an S-S link has six design variables, those being the coordinates of the two S joints. This means that up to six copies of Eq. 7, each having a different desired wheel motion, can be used to find the link geometry. This amounts to a maximum of seven specifiable wheel positions (design position plus the other six reached by the wheel motions). The maximum number of specifiable positions for the rest of the body-wheel connections are shown in Table 2. Connections not capable of achieving the minimum number of desired positions are easily eliminated prior to any further design work.

| R | C | S | S-S | R-S | R-R | S-C |
|---|---|---|---|---|---|---|
| 2* | 2 | 2* | 7 | 4 | 3 | 3 |

Tab. 2: Maximum number of specifiable positions for the practical body-wheel connections. For the R and S joints, the motion between the two positions must have a fixed point.

The specified points along the desired wheel trajectory are not limited to positions. For this application, velocity specifications are useful as well and can be specified at desired points. For example, the S-S link position equation (7) can be differentiated, yielding

$$(\boldsymbol{\omega} \times (\mathbf{A}\mathbf{x}_1 + \mathbf{b}) + \mathbf{v}) \cdot (\mathbf{A}\mathbf{x}_1 + \mathbf{b} - \mathbf{x}_0) = 0,$$

which simply prescribes that the velocity vector of the wheel-side point $(\mathbf{A}\mathbf{x}_1 + \mathbf{b})$ be perpendicular to the link. When including velocity specifications, the total number of design equations is still limited by the number of design variables.

The design equations of the connections considered here are, in general, systems of polynomial equations. For example, (7), when used for seven wheel positions, produces a system of six quadratic equations. As such, the tools of numerical algebraic geometry are useful here [12]. In particular, polynomial continuation allows a large number of link geometry solutions to be found simultaneously, so it is well-suited to this design problem. Software such as [13] provides these methods in a more-or-less "black box" format. The design equations are, in general, underdetermined, that is, there are more design variables than equations. This is generally desired by suspension designers, so that they can incorporate non-kinematic design considerations. However, handling this systematically is challenging. Most black box solvers need a determined system for solution.

## 4.2 Example: The S-S Link

An attractive choice of design equations for the S-S link has us choose design position velocity (Velocity at *Position 1*), a jounce position (*Position 2*), and a rebound position (*Position 3*). That is, we seek $\mathbf{x}_0$ and $\mathbf{x}_1$ such that

$$(\boldsymbol{\omega}_1 \times \mathbf{x}_1 + \mathbf{v}_1) \cdot (\mathbf{x}_1 - \mathbf{x}_0) = 0$$
$$\mathbf{x}_1^T (\mathbf{I} - \mathbf{A}_i^T)\mathbf{x}_0 + \mathbf{b}_i^T \mathbf{A}_i \mathbf{x}_1 - \mathbf{b}_i^T \mathbf{x}_0 + \mathbf{b}_i^T \mathbf{b}_i / 2 = 0;\ i = 2,3.$$

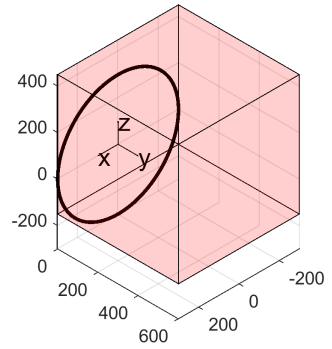


Fig. 3: Package space allotted for the S-S link synthesis example.

The second of these arises from algebraic manipulation of (7). This facilitates writing the combined design equations as

$$\begin{pmatrix} (\boldsymbol{\omega}_1 \times \mathbf{x}_1 + \mathbf{v}_1)^T \\ (\mathbf{b}_2 - (\mathbf{I} - \mathbf{A}_2)\mathbf{x}_1)^T \\ (\mathbf{b}_3 - (\mathbf{I} - \mathbf{A}_3)\mathbf{x}_1)^T \end{pmatrix} \mathbf{x}_0 = \begin{pmatrix} (\boldsymbol{\omega}_1 \times \mathbf{x}_1 + \mathbf{v}_1)^T \mathbf{x}_1 \\ \mathbf{b}_2^T(\mathbf{A}_2\mathbf{x}_1 + \mathbf{b}_2/2) \\ \mathbf{b}_3^T(\mathbf{A}_3\mathbf{x}_1 + \mathbf{b}_3/2) \end{pmatrix}.$$

Consequently, for a choice of wheel-side S joint coordinate $\mathbf{x}_1$, we can find body-side S joint coordinate $\mathbf{x}_0$ by solving a system of *linear* equations.

In this example, we use our previously-defined rear wheel trajectory. Positions 2 and 3 are chosen as those of $z = \pm 25$ mm, respectively. To three significant figures,

$$\boldsymbol{\omega}_1 = \begin{pmatrix} -0.344 \\ 0.543 \\ 0.0873 \end{pmatrix} \times 10^{-3} \text{ [mm}^{-1}\text{]} \text{ and } \mathbf{v}_1 = \begin{pmatrix} -0.105 \\ -0.0398 \\ 1.00 \end{pmatrix}.$$

The second wheel position has, to three significant figures,

$$\begin{pmatrix} \phi \\ \gamma \\ \delta \end{pmatrix} = \begin{pmatrix} 0.0136 \\ -0.00953 \\ 0.00218 \end{pmatrix} \text{ and } \mathbf{b}_2 = \begin{pmatrix} -2.63 \\ -0.257 \\ 25.0 \end{pmatrix} \text{ [mm]},$$

while the third wheel position has, again to three significant figures,

$$\begin{pmatrix} \phi \\ \gamma \\ \delta \end{pmatrix} = \begin{pmatrix} -0.0135 \\ 0.00765 \\ -0.00218 \end{pmatrix} \text{ and } \mathbf{b}_3 = \begin{pmatrix} 2.63 \\ 1.74 \\ -25.0 \end{pmatrix} \text{ [mm]}.$$

In order for the design equations to be linear, we must specify wheel-side S joint $\mathbf{x}_1$. The strategy here is to establish a package space, discretize it, and solve for $\mathbf{x}_0$ for every discretized point in the space. The solutions for $\mathbf{x}_0$ which do not fit inside the space can then be discarded, leaving the solutions which satisfy both the design equations and the package space requirement. Here, the package space is chosen as the coordinate vectors

$$\{(x,y,z)^T \in \mathbb{R}^3 : -300 \leq x \leq 300, 0 \leq y \leq 600, -150 \leq z \leq 450\}.$$

This is a cube with dimension 600 mm, equal to the tire's diameter, as seen in Figure 3. The cube is easily discretized by considering 1 mm increments along each dimension, giving $601^3$ or approximately 217 million grid points. Package spaces more interesting than a cube could of course be considered without much difficulty, but a cube suffices here.

MATLAB R2017b was employed as the software platform. The only case where the design equations had a singular matrix was when $\mathbf{x}_1 = \mathbf{0}$; consequently, $601^3 - 1$ link solutions were found. Of these, $4,011,018$, or

about 1.8%, fit inside the box. This set of packageable solutions is denoted by $S$. The solve process, including filtering based on package space, took about half an hour running in parallel on a 2014-model 2.20 GHz quad-core notebook PC. It is hardly practical to visualize or work directly with $S$, due to its cardinality (four million plus!). Instead, we must think of $S$ as a rich family of solutions we can increasingly filter until only what we prefer remains (the set-based design approach).

Why not specify more of the wheel trajectory and produce a smaller family of solutions? Experience has shown that it is improbable that a "better" motion specification produces links which are packageable. For automobile suspension linkages, it seems the relevant advantage of the S-S link is not its ability to match more points and/or tangents of a wheel trajectory, but its ability to offer a uniquely large number of packageable solutions (compared to the other body-wheel connection types). These packageable solutions can then be pruned by concerns other than wheel kinematics, as presented in the next section.

# 5 Non-Kinematic Design Considerations

Non-kinematic design concerns can help to choose among the joint/link solutions in order to assemble a complete linkage. In this section, the approach is demonstrated by using the previous S-S link solutions to construct a five link, or $(\text{S-S})^5$, architecture. In constructing an architecture from individually-synthesized connections, each connection used must have been created from the same wheel positions/velocities.

## 5.1 Links Packaging Inside a Wheel

Suppose we wish the outer S joint to lie within the rim of the wheel. This space, at its simplest, can be modeled as that inside a cylinder; for example,

$$\{(x,y,z)^T \in \mathbb{R}^3 : x^2 + z^2 < r_w^2, y_{\min} < y < y_{\max}\},$$

where $r_w$ is the wheel's (inner) radius and $y_{\min}$ and $y_{\max}$ establish the depth of the available space inside the rim. For example, let $r_w = 150$ mm, $y_{\min} = 0$ mm, and $y_{\max} = 100$ mm. Searching the solutions $S$ results in a set denoted by $S_w$, $|S_w| = 135,873$.

## 5.2 Links Achieving a Certain Kingpin

To establish a steering axis, or *kingpin*, in the design position, designers may be interested in having the line through $\mathbf{x}_0$ and $\mathbf{x}_1$ intersect the desired kingpin. If a line $\ell_1$ has equation $\mathbf{r} \times \mathbf{a}_1 = \mathbf{b}_1$ and a line $\ell_2$ has equation $\mathbf{r} \times \mathbf{a}_2 = \mathbf{b}_2$, and the two lines are not parallel, then the least distance between them is equal to [14, §8.5, #9]

$$\pm \frac{\mathbf{b}_1 \cdot \mathbf{a}_2 + \mathbf{a}_1 \cdot \mathbf{b}_2}{|\mathbf{a}_1 \times \mathbf{a}_2|}. \tag{8}$$

We can compute the least distance between each link and the desired kingpin. If the distance is zero, we have a true intersection; if the distance is within some tolerance (say, 0.1 mm), then we have a *de facto* intersection. We could have included the kingpin requirement in the synthesis as it amounts to another design position velocity specification. However, in doing so, we lose either the linearity of the design equations or a desired wheel position.

Let us now translate (8) into suspension geometry terminology. If $\ell_1$ is the line through a link solution $\mathbf{x}_0$ and $\mathbf{x}_1$, then a choice for $\mathbf{a}_1$, its direction vector, is $\mathbf{x}_1 - \mathbf{x}_0$. The vector $\mathbf{b}_1$ is the *moment vector* of the line $\ell_1$, found by crossing any point on the line with the chosen direction vector. Hence, we let $\mathbf{b}_1 = \mathbf{x_1} \times (\mathbf{x}_1 - \mathbf{x}_0) = \mathbf{x}_0 \times \mathbf{x}_1$. For the kingpin, which will be line $\ell_2$, consider the geometry of Figure 4. The kingpin is given by four parameters: kingpin inclination angle $\sigma$, positive when the kingpin leans toward the vehicle body; scrub radius $r_s$, positive when the kingpin/ground intersection is inboard of the wheel center; caster angle $\tau$, positive when the kingpin

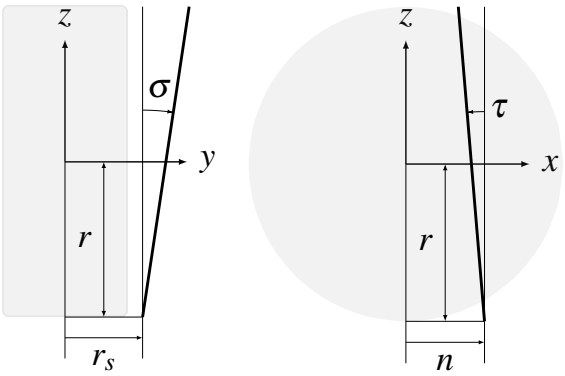


Fig. 4: Kingpin geometry definition in the design position.

leans rearward; and caster offset $n$, positive when the kingpin/ground intersection is ahead of the tire contact point. Consequently, a choice of direction vector for $\ell_2$ is

$$\mathbf{a}_2 = \begin{pmatrix} -\tan\tau \\ \tan\sigma \\ 1 \end{pmatrix}.$$

A point on the kingpin is $(n, r_s, -r)^T$; the corresponding moment vector of $\ell_2$ is

$$\mathbf{b}_2 = \begin{pmatrix} r\tan\sigma + r_s \\ r\tan\tau - n \\ r_s\tan\tau + n\tan\sigma \end{pmatrix}.$$

As an example, let us now find link solutions with the simple kingpin geometry given by $\sigma = 0$, $r_s = 0$, $\tau = 0$, and $n = 0$. Consequently, $\mathbf{a}_2 = \mathbf{k}$ and $\mathbf{b}_2 = \mathbf{0}$. We search the set $S$, yielding a set denoted by $S_k$ with cardinality 1,284. The de facto intersection tolerance was set to 0.1 mm.

### 5.3 Links Achieving the Desired Plan View Angle

Designers may have an interest in specifying the *plan view angle*, which is the angle between the S-S link and the lateral (**j**) direction when the link is projected onto a plan view (**k**-normal) plane. The plan view angle is considered positive when the body-side point $\mathbf{x}_0$ is ahead of the wheel-side point $\mathbf{x}_1$ in the plan view. The plan view angle, denoted by $\alpha$, can be computed as

$$\alpha = \arctan \frac{(\mathbf{x}_0 - \mathbf{x}_1)\cdot\mathbf{i}}{(\mathbf{x}_0 - \mathbf{x}_1)\cdot\mathbf{j}}.$$

For example, suppose we want plan view angle $\alpha_1$, where $-5^\circ \le \alpha_1 \le 0^\circ$. Searching $S$ results in the set denoted by $S_{\alpha_1}$, $|S_{\alpha_1}| = 174,759$. For the five S-S link suspension, there may be several plan view angles of interest. For $\alpha_2$, $25^\circ \le \alpha_2 \le 30^\circ$, we find $S_{\alpha_2}$, with size 146,320; whereas for $\alpha_3$, $0^\circ \le \alpha_3 \le 5^\circ$, we find $S_{\alpha_3}$, $|S_{\alpha_3}| = 170,668$.

### 5.4 Links at a Certain Coordinate

We can search for link solutions that match all or part of the desired coordinates of the S joints. For example, suppose we want solutions which have $x_1 \ge 100$ and $z_1 = 0$, where $\mathbf{x}_1 = (x_1, y_1, z_1)^T$. Searching $S$ for this condition results in the set denoted by $S_c$, with $|S_c| = 2,140$.

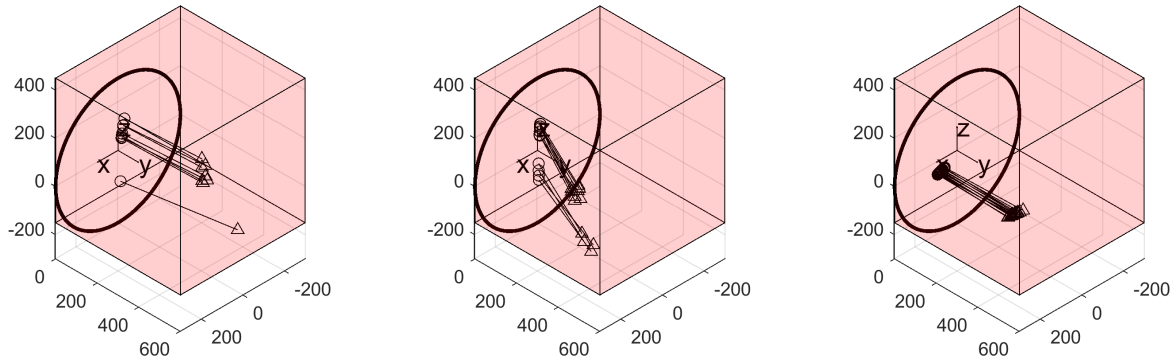


(a) Plot of the back links $S_b$. (b) Plot of the front links $S_f$. (c) Plot of the toe links $S_t$.

Fig. 5: S-S link solutions meeting the criteria for front, back, or toe links.

### 5.5 Link Types Based on Set Intersections

A typical five S-S link independent suspension linkage is constructed with a pair of upper links, a pair of lower links, and a separate fifth link [1]. Each of the upper and lower pairs aims towards the intended kingpin, with the links angling toward each other in the plan view. The fifth link, also called the toe link, is at the height of the wheel center; it can be either ahead or behind the wheel center. Here, we define *back links* as

$$S_b := S_w \cap S_k \cap S_{\alpha_1},$$

*front links* as

$$S_f := S_w \cap S_k \cap S_{\alpha_2},$$

and *toe links* as

$$S_t := S_w \cap S_{\alpha_3} \cap S_c.$$

There are 8 back links (Figure 5a), 12 front links (Figure 5b), and 14 toe links (Figure 5c). The fixed, body-side point is plotted with the triangular marker.

### 5.6 Choosing Five Links by Minimizing Reaction Loads

To reduce to the final five links, we choose five such that the reaction forces in the linkage are minimized, which could translate into less massive linkages and thus lighter suspensions. We must choose two from $S_b$, two from $S_f$, and one from $S_t$. Consequently, there are

$$(|S_b| \text{ choose } 2) \times (|S_f| \text{ choose } 2) \times |S_t| = 28 \times 66 \times 14 = 25,872$$

possible five link suspensions here. For each of these, we can determine the link reaction loads from a force at the tire contact point as follows.

Let $\mathbf{F} = (F_x, F_y, F_z)^T$ be the force at the design position tire contact point, which has coordinates $\mathbf{c}(0) = (0,0,-r)^T$. The components $F_x$ and $F_y$ are specifiable, whereas $F_z$ is an unknown. This is because we want the wheel to be in static equilibrium, when it would otherwise accelerate vertically because it has that degree-of-freedom. So we solve for $F_z$ which ensures static equilibrium. The reaction force of the $i$th link ($i = 1,2,\ldots,5$) is

$$\lambda_i(\mathbf{x}_1^{(i)} - \mathbf{x}_0^{(i)}),$$

where $\lambda_i$ is unknown. Consequently, the magnitude of the reaction force is $\lambda_i|\mathbf{x}_1^{(i)} - \mathbf{x}_0^{(i)}|$. Conditions for static equilibrium of the wheel are that the net moment about the tire contact point is zero and that the net force is zero.

Tab. 3: Coordinates of the five S-S link example (three significant figures).

| | Back Lower | Back Upper | Front Lower | Front Upper | Toe |
|---|---|---|---|---|---|
| $x_0$ | $-46.0$ | $-25.0$ | 261 | 214 | 170 |
| $y_0$ | 530 | 378 | 519 | 378 | 415 |
| $z_0$ | $-88.1$ | 142 | $-29.6$ | 138 | 14.2 |
| $x_1$ | $-1.00$ | $-2.00$ | 7.00 | 17.0 | 143 |
| $y_1$ | 11.0 | 29.0 | 14.0 | 30.0 | 53.0 |
| $z_1$ | $-123$ | 146 | $-112$ | 134 | 0.00 |

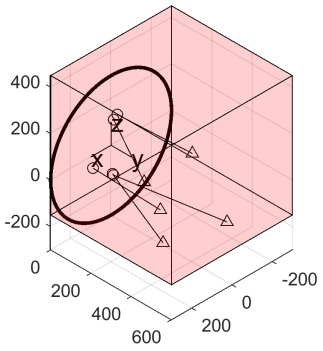


Fig. 6: Plot of the assembled five S-S link suspension.

The first of these conditions gives us the equations

$$\sum_{i=1}^{5}(\mathbf{x}_1^{(i)} - \mathbf{c}(0)) \times \lambda_i(\mathbf{x}_1^{(i)} - \mathbf{x}_0^{(i)}) = \mathbf{0},$$

while the second static equilibrium condition gives us the equations

$$\mathbf{F} + \sum_{i=1}^{5} \lambda_i(\mathbf{x}_1^{(i)} - \mathbf{x}_0^{(i)}) = \mathbf{0}.$$

All together, this is a system of six linear equations with six unknowns $\lambda_1, \ldots, \lambda_5$ and $F_z$. After solving, we compute the *cost*, defined as

$$\sum_{i=1}^{5}(\lambda_i|\mathbf{x}_1^{(i)} - \mathbf{x}_0^{(i)}|)^2.$$

That is, the sum of the squares of the reaction force magnitudes. Once we have the cost for each of the possible choices of five links, we choose the one with minimum cost.

Here, we select $F_x = -1000$ N and $F_y = 1000$ N; that is, we optimize the linkage for a combined braking and cornering load. The coordinates of the linkage are given in Table 3; the linkage is plotted in Figure 6.

# 6 Analysis of the Synthesized Suspensions

The synthesized suspensions need to be analyzed in order to ensure they guide the wheel as desired. We demonstrate the approach with the $(\text{S-S})^5$ example. The S-S equation for position, (7) or its equivalent, can be used for each link, resulting in a nonlinear system of equations having five unknowns $\phi$, $\gamma$, $\delta$, $x$, and $y$ for a given $z$ value.

The system

$$\begin{pmatrix} \left(\mathbf{x}_1^{(1)}\right)^T (\mathbf{I}-\mathbf{A}^T)\mathbf{x}_0^{(1)} + \mathbf{b}^T\mathbf{A}\mathbf{x}_1^{(1)} - \mathbf{b}^T\mathbf{x}_0^{(1)} + \mathbf{b}^T\mathbf{b}/2 \\ \left(\mathbf{x}_1^{(2)}\right)^T (\mathbf{I}-\mathbf{A}^T)\mathbf{x}_0^{(2)} + \mathbf{b}^T\mathbf{A}\mathbf{x}_1^{(2)} - \mathbf{b}^T\mathbf{x}_0^{(2)} + \mathbf{b}^T\mathbf{b}/2 \\ \vdots \\ \left(\mathbf{x}_1^{(5)}\right)^T (\mathbf{I}-\mathbf{A}^T)\mathbf{x}_0^{(5)} + \mathbf{b}^T\mathbf{A}\mathbf{x}_1^{(5)} - \mathbf{b}^T\mathbf{x}_0^{(5)} + \mathbf{b}^T\mathbf{b}/2 \end{pmatrix} = \mathbf{0}$$

is easily solved (with Newton's method). The derivative of this equation is easily solved during this process as well, allowing velocity characteristic curves to be constructed. The same method works for other body-wheel connections.

Despite only specifying design position velocity and the two positions of $z = \pm 25$, the synthesized five link suspension produces wheel motion very close to desired — it is difficult to tell the actual versus desired curves apart in the plots. Camber results are shown in Figure 7a. Toe results, Figure 7b. For wheel-travel angle, see Figure 7c. Support angle is shown in Figure 7d. For roll center height results, see Figure 7e. The five link suspension offers excellent kinematic performance and considerable non-kinematic flexibility.

# 7 Closing Remarks

Overall, this paper presents a set of mathematical tools useful for specifying complete wheel trajectories, enumerating suspension linkages, solving for suspension geometry, and satisfying non-kinematic design considerations. In particular, the wheel motion formalism makes clear the compromises inherent in stating how a wheel should move with respect to a vehicle body. For instance, roll center height $h$ is dependent on wheel center lateral displacement $y$ and so only one can be set independently. As such, with this motion formalism, suspension designers are well-equipped to develop feasible wheel motion requirements before ever selecting a particular mechanism. While the joint/link catalog here is practical, not exhaustive, other connections can be included, and the approach of generating potential architectures is sound, as is the approach for dimensional synthesis, if those connections produce algebraic design equations. Even though the S-S link example here focuses on design equations which are linear, those which are polynomial can be solved using the aforementioned methods. Despite being unable to include every non-kinematic design possibility, methods similar to those used for the S-S link can be constructed and applied in order include additional body-wheel connections in a comprehensive, set-based design process. Unfortunately, for the simpler connections, such as the R, S, and C joints, it is virtually impossible to include non-kinematic considerations; the design position wheel velocity essentially determines these geometries completely. The desire to articulate such issues formally, so that the offending design solutions can be eliminated as early as possible in the design process, was the driving force behind the development of these methods.

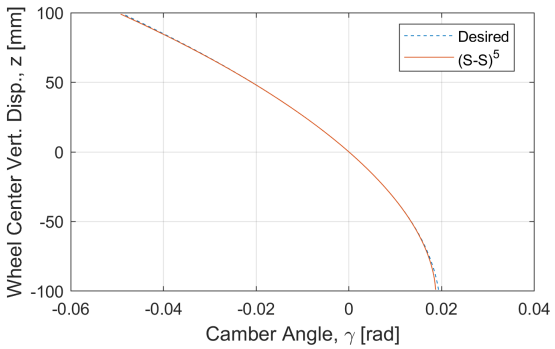


(a) Camber curve for the synthesized five link suspension.

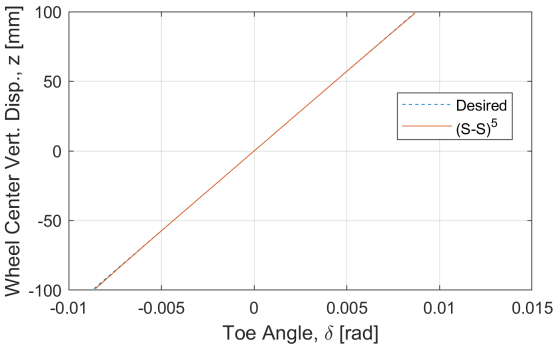


(b) Toe curve for the synthesized five link suspension.

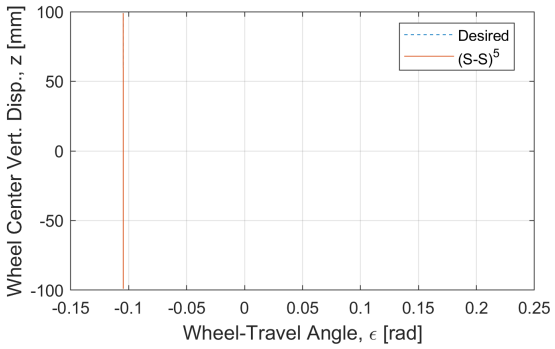


(c) Wheel-travel angle curve for the synthesized five link suspension.

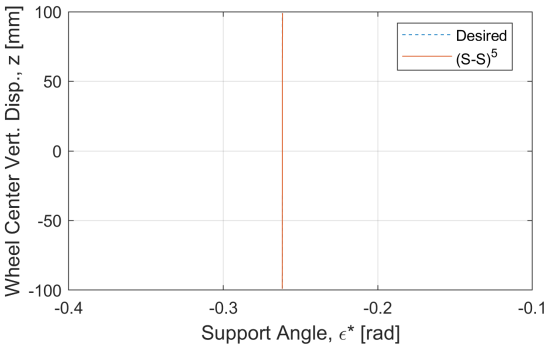


(d) Support angle curve for the synthesized five link suspension.

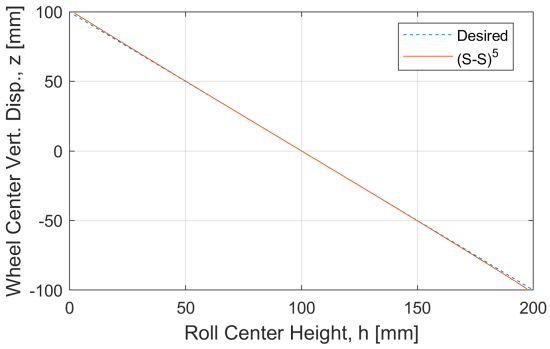


(e) Roll center height curve for the synthesized five link suspension.

Fig. 7: Wheel-travel curves for the synthesized (S-S)$^5$ suspension overlaid on the desired wheel trajectory.

# References


[1] B. Heißing and M. Ersoy, *Chassis Handbook*. Vieweg+Teibner Verlag, 2011.

[2] M. Raghavan, "Suspension design for linear toe curves: A case study in mechanism synthesis," *Journal of Mechanical Design*, vol. 126, pp. 279–282, 2004.

[3] C. H. Suh and C. W. Radcliffe, *Kinematics and Mechanisms Design*. Wiley, 1978.

[4] J. M. McCarthy and G. S. Soh, *Geometric Design of Linkages*. Springer, Second Edition, 2011.

[5] M. Raghavan, "An atlas of linkages for independent suspensions," Tech. Rep. 911925, Society of Automotive Engineers, Inc., 1991.

[6] M. B. Gerrard, "Kinematic suspension linkages - a model for their behaviour and a procedure for their design," Tech. Rep. 2002-01-0281, Society of Automotive Engineers, Inc., 2002.

[7] C. H. Suh, "Synthesis and analysis of suspension mechanisms with use of displacement matrices," Tech. Rep. 890098, Society of Automotive Engineers, Inc., 1989.

[8] M. Raghavan, "Number and dimensional synthesis of independent suspension mechanisms," *Mechanism and Machine Theory*, vol. 31, pp. 1141–1153, 1996.

[9] M. Raghavan, "Suspension synthesis for n:1 roll center motion," *Journal of Mechanical Design*, vol. 127, pp. 673–678, 2005.

[10] W. Milliken and D. Milliken, *Race Car Vehicle Dynamics*. Society of Automotive Engineers, Inc., 1995.

[11] W. Matschinsky, *Road Vehicle Suspensions*. Professional Engineering Publishing, 2000.

[12] C. W. Wampler and A. J. Sommese, "Numerical algebraic geometry and algebraic kinematics," *Acta Numerica*, vol. 20, pp. 469–567, 2011.

[13] D. J. Bates, J. D. Hauenstein, A. J. Sommese, and C. W. Wampler, "Bertini: Software for numerical algebraic geometry," 2013.

[14] J. Roe, *Elementary Geometry*. Oxford Science Publications, 1993.